

Hybrid Prefactor Semiclassical Initial Value Series Representation of the Quantum Propagator

Shesheng Zhang and Eli Pollak*

Chemical Physics Department, Weizmann Institute of Science, 76100 Rehovot, Israel

Received October 28, 2004

Abstract: One of the central advantages of the Herman Kluk Semiclassical Initial Value Representation (SCIVR) of the quantum propagator is that through its prefactor it approximately conserves unitarity for relatively long times. Its main disadvantage is that the prefactor appearing in the SCIVR propagator is expensive to compute as the dimensionality of the problem increases. When using the SCIVR series method for computation of the numerically exact quantum dynamics, the expense becomes even larger, since each term in the series involves a product of propagators, each with its own prefactor. This expense can be eliminated if one uses prefactor free propagators; however, these do not conserve unitarity as well as the HK propagator. As a compromise, we suggest the use of a hybrid propagator, in which the system variables are treated with the Herman–Kluk prefactor, while the bath variables are treated as prefactor free. Numerical application to a quartic oscillator coupled bilinearly to five harmonic bath oscillators demonstrates the viability of the hybrid method. The results presented are also a first application of the SCIVR series method to a system with six degrees of freedom. Convergence to the numerically exact answer using Monte Carlo sampling is obtained with at most the first two terms in the SCIVR series.

I. Introduction

The semiclassical initial value representation (SCIVR) approximation to the exact quantum propagator^{1–3} has been demonstrated to be a practical way of approximately computing quantum mechanical effects through classical molecular dynamics simulations in systems with “many” degrees of freedom.^{4–18} The most widely used SCIVR form is that suggested by Herman and Kluk (HK) in 1984.³ Over a decade ago, Kay demonstrated^{5–7} that one may use the HK approximation for the propagator and obtain reasonably good results, when compared to numerically exact quantum computations on small systems. This led to an increasing number of studies of the semiclassical IVR method, including applications to systems with many degrees of freedom.^{22,23} Recent reviews may be found in refs 19–21.

A major difficulty though in the application of the HK method is the computation of the prefactor.^{12,14,24–27} It is a square root of a determinant of a complex linear combination

of matrices and as such must be computed at each time step to ensure continuity of its phase. For a system with N degrees of freedom, one must integrate not only the $2N$ equations of motion in phase space but also the $(2N)^2$ time dependent monodromy matrix elements. Moreover, because the HK prefactor is in the numerator, classical chaotic motion can lead to an exponentially increasing prefactor making the Monte Carlo computation virtually impossible.²⁵

One way of overcoming these problems is by using prefactor free propagators,^{28,33–35} of which Heller’s frozen Gaussian is the first example.² However the HK propagator was invented by Herman and Kluk among others to precisely solve an acute problem which appears in the frozen Gaussian propagator. It rapidly loses unitarity.

In recent years, we have developed the SCIVR series method^{29–33,36,37} which uses the SCIVR propagator to obtain *exact* quantum propagation. In this formalism, the SCIVR propagator is the zeroth-order term in a perturbation series where the “small” perturbation is a “correction operator”²⁹ whose explicit form depends on the choice of the zeroth-

* Corresponding author e-mail: eli.pollak@weizmann.ac.il.

order SCIVR propagator. The SCIVR series method has been applied successfully to a number of problems, including one-dimensional motion on an anharmonic potential,^{31,32} “deep” tunneling through a symmetric Eckart barrier,³⁶ the interference pattern of a Gaussian wave packet scattered through a two-dimensional double slit potential,³³ and more. In all these studies, only a few terms in the SCIVR series were needed to compute the numerically exact result, demonstrating that one could use Monte Carlo methods to converge real time quantum dynamics computations.

In the SCIVR series method, the computational price of each additional term in the series is heavy, as the n -th term involves a product of $n + 1$ propagators and n time integrations. One is thus interested in reducing the integration time of the underlying classical dynamics to a minimum. It is at this point, where again the HK prefactor presents a challenge due to the expense involved in its computation. We also note, that thus far the SCIVR series method has been applied at most to systems with two degrees of freedom.

In this paper we present a new method, which is based on a hybrid between the HK propagator and the prefactor free propagator.³³ The method should be especially useful for dissipative systems, that is systems which are bilinearly coupled to harmonic baths. The idea is to use the HK prefactor for the system degrees of freedom but to use the prefactor free method for the bath degrees of freedom. In Section II we derive the hybrid propagator and its associated correction operator by demanding that on the average the contribution from the bath degrees of freedom to the correction operator vanishes.

In Section III we apply this methodology and compare it with the HK based SCIVR series method for a particle moving in a quartic potential but coupled bilinearly to a bath of five harmonic oscillators. We find that the unitarity of the hybrid propagator is substantially improved as compared to the prefactor free propagator. This is also the first example of the application of the SCIVR series method to a problem with six degrees of freedom. The results presented show convergence using only the first two terms of the SCIVR series. We end the paper in Section IV with a Discussion of the results and future applications.

II. A Hybrid SCIVR Propagator

A. The SCIVR Series Method. Briefly, we review first the SCIVR series formalism. The exact quantum propagator $\hat{K}(t)$ obeys the equation of motion

$$i\hbar \frac{\partial}{\partial t} \hat{K}(t) = \hat{H} \hat{K}(t), \hat{K}(0) = \hat{I} \quad (2.1)$$

while the SCIVR propagator $\hat{K}_0(t)$ equation of motion has the general form:²⁹

$$i\hbar \frac{\partial}{\partial t} \hat{K}_0(t) = \hat{H} \hat{K}_0(t) + \hat{C}(t), \hat{K}_0(0) = \hat{I} \quad (2.2)$$

Here, \hat{H} is the Hamiltonian operator and $\hat{C}(t)$ is termed the “correction operator”. The formal solution for the SCIVR propagator is then readily seen to be³²

$$\hat{K}_0(t - t_i) = \hat{K}(t - t_i) - \frac{i}{\hbar} \int_{t_i}^t dt' \hat{K}(t - t') \hat{C}(t') \quad (2.3)$$

We may now represent the exact propagator in terms of a series, in which the j -th element is of the order of $\hat{C}(t)^j$:

$$\hat{K}(t - t_i) = \sum_{j=0}^{\infty} \hat{K}_j(t - t_i) \quad (2.4)$$

Inserting the series expansion into the formal solution 2.3 one finds the recursion relation:

$$\hat{K}_{j+1}(t - t_i) = \frac{i}{\hbar} \int_{t_i}^t dt' \hat{K}_j(t - t') \hat{C}(t') \quad (2.5)$$

This recursion relation together with the known form of the correction operator provides a series representation of the exact propagator. Past experience has shown that this series typically converges rapidly. In the next subsection we shall derive the hybrid SCIVR propagator and its associated correction operator.

B. The Hybrid SCIVR Propagator. We assume that we are dealing with a system with N_s degrees of freedom and a bath with $N_b = N - N_s$ degrees of freedom. The classical phase space (with mass weighted coordinates and momenta) may be separated into the system phase space $\mathbf{p}_s = (p_1, p_2, \dots, p_{N_s})$, $\mathbf{q}_s = (q_1, q_2, \dots, q_{N_s})$, and bath phase space $\mathbf{p}_b = (p_{N_s+1}, p_{N_s+2}, \dots, p_N)$, $\mathbf{q}_b = (q_{N_s+1}, q_{N_s+2}, \dots, q_N)$. We will further use the notation $\mathbf{Y}_s = (\mathbf{p}_s, \mathbf{q}_s)$, $\mathbf{Y}_b = (\mathbf{p}_b, \mathbf{q}_b)$, $\mathbf{Y} = (\mathbf{Y}_s, \mathbf{Y}_b)$. We assume that the Hamiltonian may be subdivided into two parts, a system dependent part only and then all the rest

$$\hat{H}(\mathbf{Y}) = \hat{H}_s(\mathbf{Y}_s) + \hat{H}_{b,s}(\mathbf{Y}) = \hat{T}_s + \hat{V}_s(\mathbf{Y}_s) + \hat{T}_b + \hat{V}_{b,s}(\mathbf{Y}) \quad (2.6)$$

where \hat{T} and \hat{V} are the kinetic and potential operators, respectively. The hybrid SCIVR propagator will be defined rather generally by introducing a function $f(\mathbf{Y}, t)$ such that initially $f(\mathbf{Y}, 0) = 1$:

$$\hat{K}_0(t) = \int_{-\infty}^{\infty} \frac{d\mathbf{Y}}{(2\pi\hbar)^N} R(\mathbf{Y}_s, t) f(\mathbf{Y}, t) e^{(i/\hbar)S_s(\mathbf{Y}_s, t)} |g(\mathbf{Y}, t)\rangle \langle g(\mathbf{Y}, 0)| \quad (2.7)$$

Here, $R(\mathbf{Y}_s, t)$ is taken to be the Herman–Kluk preexponential factor, defined though on the phase space $\{\mathbf{Y}_s\}$ only. It does depend on the full phase space, in the sense that the trajectories used to generate it are trajectories in the full phase space of the combined system and bath. Its initial time value is unity $R(\mathbf{Y}_s, 0) = 1$. The classical action $S(\mathbf{Y}_s, t)$ is defined on the system phase space $\{\mathbf{Y}_s\}$ as

$$S_s(\mathbf{Y}_s, t) = \int_0^t dt' [\mathbf{p}_s(t') \dot{\mathbf{q}}_s(t') - H_s(\mathbf{Y}_s(t'))] \quad (2.8)$$

however it too depends on the full phase space in the sense that the trajectories used to evaluate the system action are propagated in the full phase space of the system and the bath. The coordinate representation of the coherent state in eq 2.7 takes the form

$$\langle \mathbf{x} | g(\mathbf{p}, \mathbf{q}, t) \rangle = \left(\frac{\det(\mathbf{\Gamma})}{\pi^N} \right)^{1/4} \exp \left[- (1/2) [\mathbf{x} - \mathbf{q}_t]^T \mathbf{\Gamma} [\mathbf{x} - \mathbf{q}_t] + \frac{i}{\hbar} \mathbf{p}_t \cdot (\mathbf{x} - \mathbf{q}_t) \right] \quad (2.9)$$

and $\mathbf{\Gamma}$ in this paper will be defined as a *diagonal* time independent width parameter matrix so that it may be divided into two submatrices $\mathbf{\Gamma}_s$ for the system degrees of freedom and $\mathbf{\Gamma}_b$ for the bath degrees of freedom. With these definitions one notes that at time $t = 0$, the generalized hybrid SCIVR propagator of eq 2.7 is the identity matrix. The time dependence in the coherent state is obtained from Hamilton's equations of motion for the classical limit of the quantum Hamiltonian operator.

By expressly taking the time derivative of the hybrid SCIVR propagator and using Hamilton's equations of motion one derives the following expression for the correction operator

$$\hat{C}(t) = \int_{-\infty}^{\infty} \frac{d\mathbf{Y}}{(2\pi\hbar)^N} [\Delta V_s(\hat{\mathbf{q}}_s, t) + \Delta V_{b,s}(\hat{\mathbf{q}}, t)] R(\mathbf{Y}_s, t) f(\mathbf{Y}, t) e^{(i/\hbar)S_s(\mathbf{Y}_s, t)} |g(\mathbf{Y}, t)\rangle \langle g(\mathbf{Y}, 0)| \quad (2.10)$$

where the potential difference operators are

$$\Delta V_s(\hat{\mathbf{q}}_s, t) = i\hbar \frac{\dot{R}}{R} + V_s(\mathbf{Y}_s, t) + \nabla_s V_s[\mathbf{q}_s(t)] \cdot (\hat{\mathbf{q}}_s - \mathbf{q}_s(t)) - V_s(\hat{\mathbf{q}}_s) - \frac{\hbar^2}{2} Tr[\mathbf{\Gamma}_s] + \frac{\hbar^2}{2} (\hat{\mathbf{q}}_s - \mathbf{q}_s(t))^T \mathbf{\Gamma}_s (\hat{\mathbf{q}}_s - \mathbf{q}_s(t)) \quad (2.11)$$

$$\Delta V_{b,s}(\hat{\mathbf{q}}, t) = i\hbar \frac{\dot{f}}{f} + \frac{1}{2} \mathbf{p}_b(t)^T \cdot \mathbf{p}_b(t) + \nabla V_{b,s}[\mathbf{q}(t)] \cdot (\hat{\mathbf{q}} - \mathbf{q}(t)) - V_{b,s}(\hat{\mathbf{q}}) - \frac{\hbar^2}{2} Tr[\mathbf{\Gamma}_b] + \frac{\hbar^2}{2} (\hat{\mathbf{q}}_b - \mathbf{q}_b(t))^T \mathbf{\Gamma}_b (\hat{\mathbf{q}}_b - \mathbf{q}_b(t)) \quad (2.12)$$

∇_s is the gradient operator defined on the subspace of the system coordinates, and ∇ is defined on the full space of the system and the bath coordinates.

The function f has yet to be determined. As in our previous derivation of prefactor free propagators,³³ we will define it by demanding that on the average, at any point and time in the full phase space $\{Y\}$, the part of the correction operator associated with the bath will vanish. That is we define f by demanding

$$\langle g(\mathbf{Y}, t) | \Delta \hat{V}_{b,s}(\hat{\mathbf{q}}, t) | g(\mathbf{Y}, t) \rangle = 0 \quad (2.13)$$

From eq 2.12 one then finds that the solution for f is

$$f(\mathbf{Y}, t) = \exp \left(\frac{i}{\hbar} S_{b,s}(\mathbf{Y}, t) \right) \quad (2.14)$$

and the bath-system action $S_{b,s}$ is found to be

$$S_{b,s}(\mathbf{Y}, t) = \int_0^t dt' \left(\frac{1}{2} \mathbf{p}_b(t')^T \cdot \mathbf{p}_b(t') - \tilde{V}_{b,s}(\mathbf{q}(t')) - \frac{\hbar^2}{4} Tr[\mathbf{\Gamma}_b] \right) \quad (2.15)$$

The coherent state bath-system averaged potential is defined as

$$\tilde{V}_{b,s}(\mathbf{q}(t)) = \left(\frac{\det[\mathbf{\Gamma}_b]}{\pi^N} \right)^{1/2} \int_{-\infty}^{\infty} d\mathbf{x} e^{-[\mathbf{x} - \mathbf{q}(t)]^T \mathbf{\Gamma} [\mathbf{x} - \mathbf{q}(t)]} V_{b,s}(\mathbf{x}) \quad (2.16)$$

Having defined the function f we can now insert it back into the original definition of the SCIVR propagator 2.7 to get the central formal results of this paper. The zeroth-order hybrid propagator is

$$\hat{K}_0(t) = \int_{-\infty}^{\infty} \frac{d\mathbf{Y}}{(2\pi\hbar)^N} R(\mathbf{Y}_s, t) e^{(i/\hbar)[S_s(\mathbf{Y}_s, t) + S_{b,s}(\mathbf{Y}, t)]} |g(\mathbf{Y}, t)\rangle \langle g(\mathbf{Y}, 0)| \quad (2.17)$$

and the associated correction operator takes the form

$$\hat{C}(t) = \int_{-\infty}^{\infty} \frac{d\mathbf{Y}}{(2\pi\hbar)^N} R(\mathbf{Y}_s, t) e^{(i/\hbar)[S_s(\mathbf{Y}_s, t) + S_{b,s}(\mathbf{Y}, t)]} \Delta V(\hat{\mathbf{q}}, t) |g(\mathbf{Y}, t)\rangle \langle g(\mathbf{Y}, 0)| \quad (2.18)$$

The potential difference operator is

$$\Delta V(\hat{\mathbf{q}}, t) = \Delta V_s(\hat{\mathbf{q}}_s, t) + \Delta V_{b,s}(\hat{\mathbf{q}}, t) \quad (2.19)$$

$$\Delta V_s(\hat{\mathbf{q}}_s, t) = i\hbar \frac{\dot{R}}{R} + V_s(\mathbf{Y}_s, t) + \nabla_s V_s[\mathbf{q}_s(t)] \cdot (\hat{\mathbf{q}}_s - \mathbf{q}_s(t)) - V_s(\hat{\mathbf{q}}_s) - \frac{\hbar^2}{2} Tr[\mathbf{\Gamma}_s] + \frac{\hbar^2}{2} (\hat{\mathbf{q}}_s - \mathbf{q}_s(t))^T \mathbf{\Gamma}_s (\hat{\mathbf{q}}_s - \mathbf{q}_s(t)) \quad (2.20)$$

$$\Delta V_{b,s}(\hat{\mathbf{q}}, t) = \tilde{V}_{b,s}(\mathbf{q}(t)) + \nabla V_{b,s}[\mathbf{q}(t)] \cdot (\hat{\mathbf{q}} - \mathbf{q}(t)) - V_{b,s}(\hat{\mathbf{q}}) - \frac{\hbar^2}{4} Tr[\mathbf{\Gamma}_b] + \frac{\hbar^2}{2} (\hat{\mathbf{q}}_b - \mathbf{q}_b(t))^T \mathbf{\Gamma}_b (\hat{\mathbf{q}}_b - \mathbf{q}_b(t)) \quad (2.21)$$

To complete the formulation we write down here the explicit expression for the Herman–Kluk prefactor

$$R(\mathbf{Y}_s, t) = \left(\det \left[\frac{1}{2} \left(\frac{\partial \mathbf{q}_t}{\partial \mathbf{q}} + \frac{\partial \mathbf{p}_t}{\partial \mathbf{p}} - i\hbar \mathbf{\Gamma}_s \frac{\partial \mathbf{q}_t}{\partial \mathbf{p}} + \frac{i}{\hbar} \mathbf{\Gamma}_s^{-1} \frac{\partial \mathbf{p}_t}{\partial \mathbf{q}} \right) \right] \right)^{1/2} \quad (2.22)$$

where the various terms in the brackets are the four matrices for the system variables only.

We note, that in the limit that there are no bath variables, that is $N = N_s$ then the hybrid propagator and associated correction operator are identical to the Herman–Kluk propagator and correction operator. Conversely, if all degrees of freedom are considered as the bath degrees of freedom, that is $N = N_b$, then the hybrid propagator and correction operator reduces to the prefactor free frozen Gaussian propagator of Heller and its associated correction operator.

III. Application to a Dissipative System

A. Preliminaries. As a test of the hybrid method, we studied a dissipative system of a quartic double well potential ($N_s = 1$)

$$V_s(q) = -\frac{1}{2} q^2 \left(1 - \frac{q^2}{2q_a^2} \right) \quad (3.1)$$

coupled bilinearly to a bath of harmonic oscillators

$$V_{b,s}(\mathbf{q}) = \sum_{j=1}^{N_b} \frac{1}{2} \left(\omega_j x_j - \frac{c_j}{\omega_j} \right)^2 \quad (3.2)$$

The frequencies and coupling coefficients of the harmonic bath are chosen so as to mimic a cutoff bath with cutoff frequency ω_c and friction coefficient η so that the spectral density is

$$J(\omega) = \frac{\pi \sum_{j=1}^{N_b} c_j^2}{2\omega_j} \delta(\omega - \omega_j) = \eta \omega \exp^{-\omega/\omega_c} \quad (3.3)$$

The discretization for a finite number of oscillators is carried out as suggested by Gelabert et al.¹³ For the specific case of the exponential cutoff bath, this means that

$$\omega_j = -\omega_c \log \left[1 - \frac{j}{N_b} \left(1 - \exp \left(-\frac{\omega_m}{\omega_c} \right) \right) \right] \quad (3.4)$$

$$c_j = \omega_j \sqrt{\frac{2\eta\omega_c}{\pi N_b} \left[1 - \exp \left(-\frac{\omega_m}{\omega_c} \right) \right]} \quad (3.5)$$

where ω_m is the maximal bath frequency.

To simplify the numerical computation, we chose factorized initial conditions for the system and the bath. Accordingly, the initial condition for the system variable is that of a Gaussian wave packet

$$\langle q | \Psi \rangle = \left(\frac{\gamma}{\pi} \right)^{1/4} \exp \left[-\frac{\gamma}{2} (q - q_0)^2 \right] \quad (3.6)$$

The bath variables were distributed canonically with the bath Hamiltonian:

$$\hat{H}_b = \sum_{j=1}^{N_b} \frac{1}{2} (\hat{p}_j^2 + \omega_j^2 \hat{x}_j^2) \quad (3.7)$$

The actual parameters chosen in the numerical simulations are $q_0 = q_a = 2$, $\omega_c = \omega/2$, $\omega_m = 4\omega_c$, $\gamma = 10$, $\Gamma_s = 2.25$, $N_b = 5$, $T = 0$, $\Gamma_{bj} = (\omega_j/\hbar)$, and $\omega = \sqrt{2}$. The system width parameter (Γ_s) was chosen to be the optimal width for the quartic symmetric double well system, as described in ref 31.

B. Normalization. The hybrid method was invented in order to improve upon the normalization of the frozen Gaussian method without having to pay the price of computing the full monodromy matrices for system and bath. The time dependent normalization of the hybrid SCIVR propagator, using the factorized initial conditions as described above, is

$$|K_0|(t) = \sqrt{Tr_b \left[\frac{e^{-\beta \hat{H}_b}}{Q_b} \langle \Psi | \hat{K}_0^\dagger(t) \hat{K}_0(t) | \Psi \rangle \right]} \quad (3.8)$$

with $\beta = 1/k_B T$ being the inverse temperature and $Q_b = Tr_b[e^{-\beta \hat{H}_b}]$ is the partition function of the bath. Due to the choice of factorized initial conditions, the bath initial conditions are Gaussian in the bath phase space variables, while the system initial conditions are Gaussian in the system phase space variables due to the choice of the Gaussian wave packet. Therefore, the Monte Carlo computation of the normalization is straightforward.

The time dependent normalization is shown in Figure 1. These results were obtained using a Monte Carlo sample size

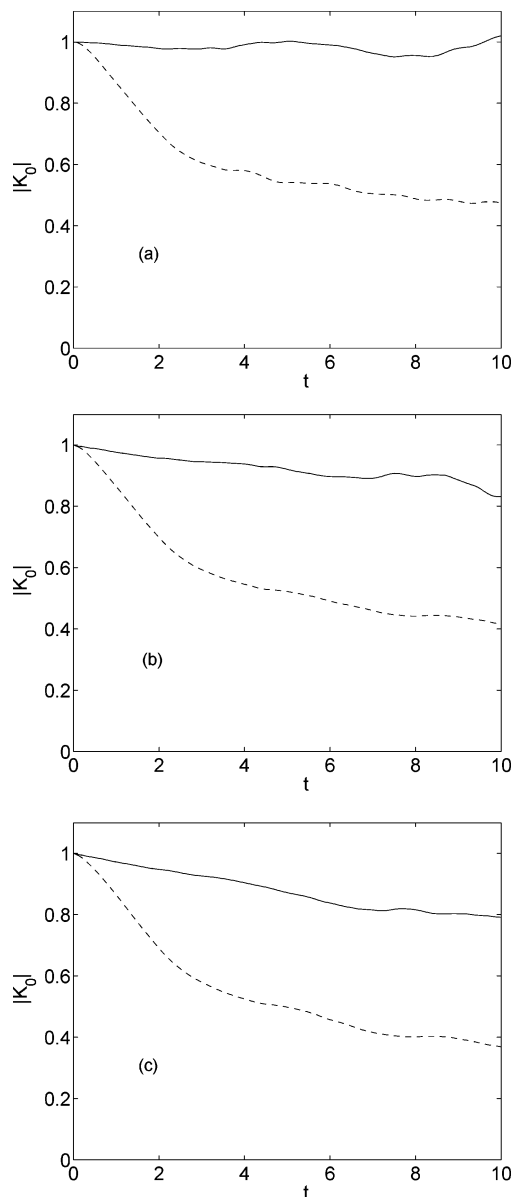


Figure 1. The time dependent normalization $|K_0|$ of the hybrid propagator for a quartic oscillator coupled bilinearly to a bath of five harmonic oscillators. Panels a–c correspond to the friction coefficient values $\eta = 0, 0.5, 3$, respectively. The solid and dashed lines correspond to the normalization obtained from the hybrid and prefactor free propagators, respectively.

of $8.1 \cdot 10^7$ for the three cases, respectively. The respective standard deviations are ≤ 0.01 . Panel a of the figure shows the normalization for the case of no system bath coupling, for which the hybrid propagator reduces to the HK system propagator, so that the unitarity presented in the figure is just a test of the unitarity of the Herman–Kluk propagator for the one-dimensional quartic oscillator. As is evident from the figure the Herman–Kluk propagator is close to unity for the whole time interval presented in the figure. Panel b shows the normalization of the hybrid propagator (solid line) for weak friction ($\eta = 0.5$) and panel c for strong friction ($\eta = 3.0$). In panels b and c we show also the normalization that would have been obtained (dashed line) had we made use of the prefactor free frozen Gaussian propagator of

Heller. As expected, use of the hybrid propagator leads to an impressive improvement in the unitarity property.

C. Thermal Overlap Function. The time dependent thermally averaged overlap function of the wave packet, which includes the first k terms in the SCIVR series, is defined as

$$A_k(t) = \text{Tr}_b \left[\frac{e^{-\beta \hat{H}_b}}{Q_b} \langle \Psi | \sum_{j=0}^k \hat{K}_j(t) | \Psi \rangle \right] \quad (3.9)$$

The absolute value of the thermal overlap function is plotted in Figure 2 for the same three values of the friction coefficient as before. Numerical details about the Monte Carlo averaging are given in the Appendix. Results are presented for both the Herman–Kluk propagator used for all degrees of freedom as well as the hybrid method, in which the HK form is used only for the system variables. The Monte Carlo sample size used for A_0 was 1.3×10^6 points, enough to ensure an accuracy of 0.01, while for A_1 1.74×10^7 points were used to keep the same accuracy. The CPU time needed for the HK propagator was about 10 times greater than the CPU time used for the hybrid propagator. As can be seen from the figure, the converged results are very close to each other, justifying the use of the hybrid method.

The results shown in Figure 2 for $\eta = 0$ have already been published in ref 31; they serve to remind us that for the system alone, we know that convergence is obtained by including only the first two terms in the series. At $\eta = 0$ we could compare the SCIVR series results with the numerically exact result as obtained from matrix diagonalization of the Hamiltonian. However, in the presence of friction we do not know the numerically exact results from an independent computation. The results in the figure show though that the differences between the zeroth-order and the first-order terms are sufficiently small even in the presence of friction so that we can safely assume that there is no need to go to higher order terms in the series. This is then the first example of the convergence of the SCIVR series method for real time dependent quantum dynamics on a system with six degrees of freedom.

D. The Thermal Autocorrelation Function. As a last example, we consider a more physically measurable quantity, the thermal autocorrelation function of the Gaussian wave packet, defined as

$$M(t) = \text{Tr} \left[\frac{e^{-\beta \hat{H}_b}}{Q_b} |\Psi\rangle\langle\Psi| \hat{K}^\dagger(t) |\Psi\rangle\langle\Psi| \hat{K}(t) \right] \quad (3.10)$$

Computation of the thermal autocorrelation function is more expensive than the overlap function since here the propagator appears twice. With respect to the SCIVR series, we will use the notation

$$M(t) = M_0(t) + \Delta_1 M(t) + \Delta_2 M(t) + \dots \quad (3.11)$$

such that $\Delta_j M(t)$ denotes the term obtained by using all terms of order \hat{C}^j in the SCIVR series. The results obtained for $M(t)$, based on the hybrid propagator, are shown in Figure 3 for the strong friction case of $\eta = 3.0$. They are compared

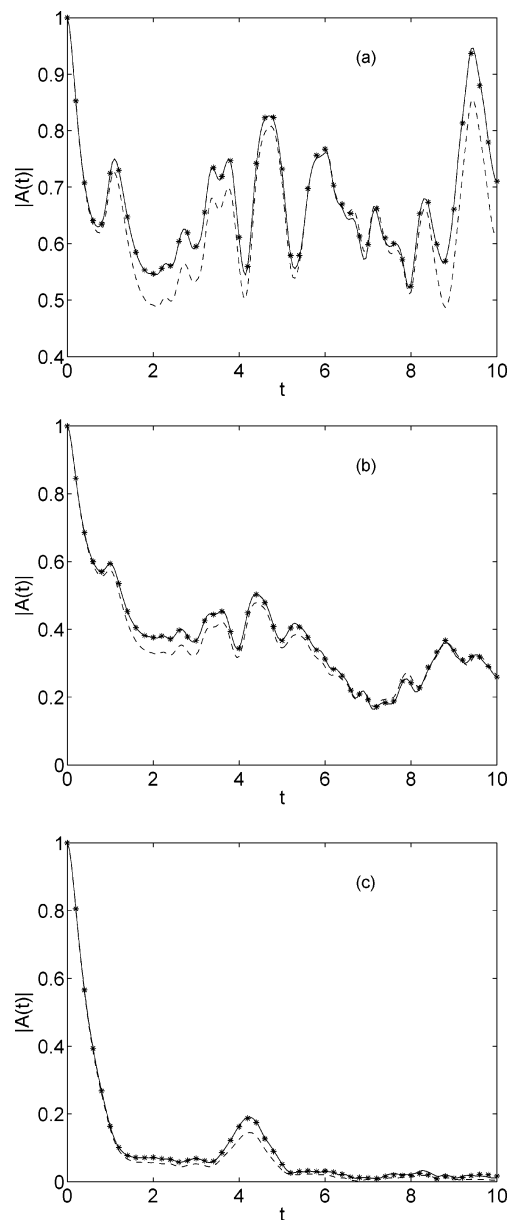


Figure 2. The time dependence of the absolute value of the thermal overlap function. Panels a–c correspond to the friction coefficient values $\eta = 0, 0.5, 3$, respectively. In all panels, the dashed and solid lines correspond to the results obtained with the zeroth-order and first-order hybrid propagator, respectively. The stars denote results obtained with the first-order HK propagator. The good agreement between the stars and the solid lines demonstrates that the hybrid propagator is as good as the HK propagator for this problem. The small differences between the zeroth-order and first-order lines indicate that the results have converged, using only the first-order term in the SCIVR series.

with the numerically exact results obtained using basis set techniques³⁸ and the “classical” autocorrelation function obtained by replacing the SCIVR dynamics with classical mechanics. From the figure we note, that here too, it suffices to go to first order in the SCIVR series. Higher order terms are negligible, in fact we also computed the second order correction up to the time $t = 7$ with no appreciable difference to that obtained with the first-order term only. Not surpris-

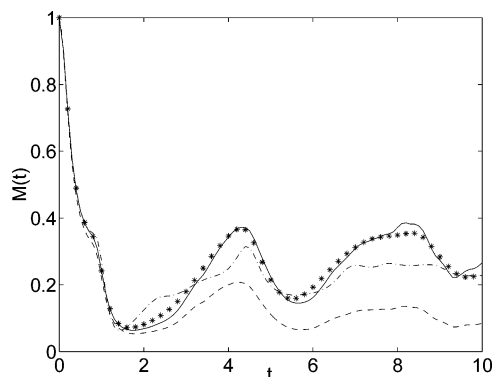


Figure 3. The time dependence of the thermal autocorrelation function for strong friction $\eta = 3.0$ using the hybrid propagator. The dashed and solid lines correspond to results obtained using the zeroth-, and zeroth-, and first-order terms in the SCIVR series, respectively. The stars are the numerically exact results of ref 38. The dashed dotted line shows the results obtained with classical mechanics propagation. Note the good agreement between the first-order SCIVR series results and the exact results.

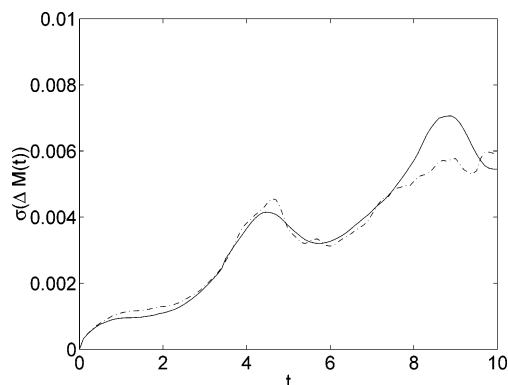


Figure 4. The time dependent variances for the leading order terms in the SCIVR series computation presented in Figure 3. The solid line is for the first-order result, the dashed-dotted line is for the zeroth-order result. The variance $\sigma(\Delta M) = \sqrt{(\langle \Delta M^2 \rangle - \langle \Delta M \rangle^2)/N}$ where N is the number of Monte Carlo points used.

ingly, we find that the deviation of the converged quantum autocorrelation function from the classical function is not very big, and at strong friction one expects dissipative quantum systems to become similar to the classical.

As for the error analysis, for M_0 we used a sample size of $6.5 \cdot 10^7$ points. For $\Delta_1 M$ the sample size was $6.8 \cdot 10^9$ points and for $\Delta_2 M$, $1.1 \cdot 10^{10}$ points. The step size in time was 0.01. The variances for the zeroth- and first-order terms are plotted in Figure 4. We note that the standard deviation for the first-order term is greater than the differences between $M_1(t)$ and the numerically exact result of ref 38.

For the thermal autocorrelation function, use of the Herman–Kluk propagator instead of the hybrid propagator would have been numerically prohibitive, the computational power of the 64 processor pentium IV PC farm at our disposal would not have been sufficient to converge the computation within a period of less than six months. The reason for this is clear. For the HK propagator, computation

of the prefactor requires the solution of $2N + 1 + (2N)^2 = 157$ coupled equations of motion for our model with $5 + 1$ degrees of freedom. For the hybrid method one needs $2N + 1 + (2N_s)^2 = 17$ coupled equations. The added expense also grows as a power law for each additional term in the SCIVR series, since each additional term requires an additional propagator with its independent prefactor. It is thus not surprising that the hybrid method leads to a considerable saving in computational time.

IV. Discussion

In this paper we have presented a new hybrid SCIVR series representation of the quantum propagator which may be considered as a compromise between the series representation based on the Herman–Kluk and the Heller prefactor free frozen Gaussian propagators. The hybrid zeroth-order propagator conserves unitarity significantly better than the Heller propagator, but the numerical effort is much smaller than that needed for the Herman–Kluk propagator. The hybrid method would seem to be ideally suited for dissipative systems where there is a clear identification of a system and a bath. Its usefulness for more general systems remains to be tested.

This paper presents also for the first time the application of the SCIVR series method to a system with 6 degrees of freedom. We found that as in our experience with one- and two-dimensional systems, the series converges rapidly and that only the first two terms in the series suffice for obtaining a converged result.

The HK propagator is known to be problematic for strongly chaotic systems, since the HK prefactor then gives an exponentially growing in time term which makes it very difficult to converge a Monte Carlo computation. The hybrid method has the potential of overcoming this problem, by judicious choice of the “system” and the “bath” so that the system part would not include the strongly chaotic trajectories.

The computations presented in this paper were for a finite time, of the order of three oscillations of the particle in a well of the quartic potential. Integration for longer times would have necessitated going to higher order terms in the SCIVR series expansion, making the computation prohibitive for our modest computational resources. We also note that all our results are for $T = 0$, which may be considered as a “tough” example as the system would tend to be more classical as the temperature is increased.

Finally, although we have used the factorization approximation for the bath, this is not essential. One may treat the full thermal Hamiltonian using imaginary time path integral methods.^{39,40} This would make the programming and computation somewhat more expensive but should not make it impossible. In this paper, we were interested to demonstrate the utility of the hybrid method and the fact that the SCIVR series can be computed and converged for “large” systems. Doing away with the factorization approximation is a topic for future work.

Acknowledgment. This work has been supported by grants from the U.S. Israel Binational Science Foundation and the Israel Science Foundation.

V. Appendix: Monte Carlo Evaluation of Terms in the SCIVR Series for the Thermal Overlap Function

In this Appendix we will describe the Monte Carlo methodology we used to evaluate the thermal overlap function. First we note that the trace of the harmonic bath Hamiltonian and the initial Gaussian wave packet with the coherent state at time t gives a Gaussian in the phase space variables at time t :

$$Tr_b[e^{-\beta\hat{H}_b}\langle\Psi|g(\mathbf{Y}, t)\rangle\langle g(\mathbf{Y}, 0)|\Psi\rangle] = \langle g(\mathbf{Y}_b, 0)|e^{-\beta\hat{H}_b}|g(\mathbf{Y}_b, t)\rangle\langle\Psi|g(\mathbf{Y}_s, t)\rangle\langle g(\mathbf{Y}_s, 0)|\Psi\rangle \quad (\text{A.1})$$

The rather lengthy analytic expression for the bath matrix element $\langle g(\mathbf{Y}_b, 0)|e^{-\beta\hat{H}_b}|g(\mathbf{Y}_b, t)\rangle$ is given in eq 3.20 of ref 13 and provides a Gaussian weighting for the initial conditions of the bath. The system term $\langle g(\mathbf{Y}_s, 0)|\Psi\rangle$ provides a Gaussian weighting for the system initial condition since

$$\langle g(\mathbf{Y}_s, t)|\Psi\rangle = \Gamma_1^{1/4} e^{-\Gamma_2(q_t - x_0)^2 - (p_t^2)/(4\Gamma_a\hbar^2) + (i)/(2\Gamma_a\hbar)p_t(q_t - x_0)} \quad (\text{A.2})$$

where $\Gamma_a = (\Gamma_s + \gamma)/2$, $\Gamma_1 = \gamma\Gamma_s/\Gamma_a^2$, $\Gamma_2 = \gamma\Gamma_s/(4\Gamma_a)$.

The computation of the leading order term is now straightforward. Each Gaussian in either coordinate or momentum is converted in standard fashion to a variable defined on the $[0, 1]$ interval and then generated randomly. One then integrates trajectories forward from time 0 to the final time and collects the data. For the leading order term one can use each time step in the integration to obtain the thermal overlap function at each intermediate time.

The first-order term is somewhat more complex, since now one has two phase space integrations, one coming from the SCIVR operator $\hat{K}_0(t)$, the other coming from the correction operator $\hat{C}(t)$. Both of them are rewritten as

$$\hat{K}_0(t - t') = \int_{-\infty}^{\infty} d\mathbf{Y} E_0(\mathbf{Y}, t - t') |g(\mathbf{Y}, t - t')\rangle \langle g(\mathbf{Y}, 0)| \quad (\text{A.3})$$

$$\hat{C}(t') = \int_{-\infty}^{\infty} d\mathbf{Y}^c E_0(\mathbf{Y}^c, t') \Delta V(\hat{\mathbf{q}}, t') |g(\mathbf{Y}^c, t')\rangle \langle g(\mathbf{Y}^c, 0)| \quad (\text{A.4})$$

and we have used the notation

$$E_0(\mathbf{Y}, t) = \frac{1}{(2\pi\hbar)^N} R(\mathbf{Y}_s, t) e^{(i/\hbar)[S_s(\mathbf{Y}_s, t) + S_{b,s}(\mathbf{Y}, t)]} \quad (\text{A.5})$$

The integrand of the first-order term may thus be rewritten as

$$Tr_b[e^{-\beta\hat{H}_b}\langle\Psi|\hat{K}_0(t - t')\hat{C}(t')|\Psi\rangle] = \int_{-\infty}^{\infty} d\mathbf{Y} \int_{-\infty}^{\infty} d\mathbf{Y}^c E_0(\mathbf{Y}, t - t') E_0(\mathbf{Y}^c, t') \times \langle g(\mathbf{Y}, 0)|\Delta V(\hat{\mathbf{q}}, t')|g(\mathbf{Y}^c, t')\rangle Tr_b[e^{-\beta\hat{H}_b}\langle\Psi|g(\mathbf{Y}, t - t')\rangle\langle g(\mathbf{Y}^c, 0)|\Psi\rangle] \quad (\text{A.6})$$

As in the case of the leading order term, the trace term in the expression is again a Gaussian in both the initial and final time phase space coordinates and momenta

$$Tr_b[e^{-\beta\hat{H}_b}\langle\Psi|g(\mathbf{Y}, t - t')\rangle\langle g(\mathbf{Y}^c, 0)|\Psi\rangle] = \langle g(\mathbf{Y}_b, 0)|e^{-\beta\hat{H}_b}|g(\mathbf{Y}_b, t - t')\rangle\langle\Psi|g(\mathbf{Y}_s, t - t')\rangle\langle g(\mathbf{Y}_s, 0)|\Psi\rangle \quad (\text{A.7})$$

thus providing a Gaussian weighting to the phase space

variables included in \mathbf{Y} and \mathbf{Y}^c . Since the phase space volume element is invariant in time ($d\mathbf{Y} = d\mathbf{Y}_t$), one can replace the integration over initial points in phase space with an integration over the final points. This then leads to Gaussian final conditions for the phase space points associated with the propagator \hat{K}_0 as well as Gaussian initial conditions for the phase space associated with the correction operator $\hat{C}(t)$. This means that for the first-order correction we have two sets of trajectories, those run backward in time associated with the SCIVR propagator and those run forward in time associated with the correction operator.

Operationally, one propagates a randomly chosen phase space point backward in time from the final time t to the initial time 0, and one has a different initial condition from which a trajectory is propagated from time 0 to time t . These two trajectories then contribute a vector of points for all the intermediate times t' . This process is then repeated a large number of times, to obtain the converged integrand which is then time integrated by Simpson's rule.

The same procedure becomes more costly when considering the integrand of the second-order contribution to the SCIVR series which now involves a product of three operators:

$$Tr_b[e^{-\beta\hat{H}_b}\langle\Psi|\hat{K}_0(t - t' - t'')\hat{C}(t'')\hat{C}(t')|\Psi\rangle] = \int_{-\infty}^{\infty} d\mathbf{Y} \int_{-\infty}^{\infty} d\mathbf{Y}'' \int_{-\infty}^{\infty} d\mathbf{Y}^c E_0(\mathbf{Y}, t - t'' - t') E_0(\mathbf{Y}'', t'') E_0(\mathbf{Y}^c, t') \langle g(\mathbf{Y}'', 0)|\Delta V(\hat{\mathbf{q}}, t')|g(\mathbf{Y}^c, t')\rangle \times \langle g(\mathbf{Y}, 0)|\Delta V(\hat{\mathbf{q}}, t'')|g(\mathbf{Y}'', t'')\rangle Tr_b[e^{-\beta\hat{H}_b}\langle\Psi|g(\mathbf{Y}, t - t'' - t')\rangle\langle g(\mathbf{Y}^c, 0)|\Psi\rangle] \quad (\text{A.8})$$

Now we have three independent phase space volumes, one coming from the propagator \hat{K}_0 , one coming from the correction operator $\hat{C}(t'')$, and the third one from $\hat{C}(t')$. As in the case of the zeroth- and first-order contributions, the term $Tr_b[e^{-\beta\hat{H}_b}\langle\Psi|g(\mathbf{Y}, t - t'' - t')\rangle\langle g(\mathbf{Y}^c, 0)|\Psi\rangle]$ is a Gaussian, providing a Gaussian weighting to two phase space volumes. However, the third intermediate Gaussian weighting results from the time dependent overlap of the two correction operators, which we write in the following form

$$\langle g(\mathbf{Y}_1, 0)|\Delta V(\hat{\mathbf{q}}, t')|g(\mathbf{Y}_2, t')\rangle = \langle g(\mathbf{Y}_1, 0)|g(\mathbf{Y}_2, t')\rangle \frac{\langle g(\mathbf{Y}_1, 0)|\Delta V(\hat{\mathbf{q}}, t')|g(\mathbf{Y}_2, t')\rangle}{\langle g(\mathbf{Y}_1, 0)|g(\mathbf{Y}_2, t')\rangle} \quad (\text{A.9})$$

The overlap of the two coherent states is known analytically and again gives a Gaussian distribution

$$\langle g(\mathbf{Y}_1, 0)|g(\mathbf{Y}_2, t')\rangle = \exp\left[-\frac{1}{4}[\mathbf{q}_1(0) - \mathbf{q}_2(t')]^T \mathbf{\Gamma} [\mathbf{q}_1(0) - \mathbf{q}_2(t')]\right] \times \exp\left[-\frac{1}{4\hbar}[\mathbf{p}_1(0) - \mathbf{p}_2(t')]^T \mathbf{\Gamma}^{-1} [\mathbf{p}_1(0) - \mathbf{p}_2(t')] + \frac{i}{2\hbar}[\mathbf{q}_1(0) - \mathbf{q}_2(t')][\mathbf{p}_1(0) + \mathbf{p}_2(t')]\right] \quad (\text{A.10})$$

The problem is that this Gaussian distribution is time dependent. Thus one can no longer run trajectories from the end and initial time points only as before and store the time dependent data between, but one has to propagate trajectories at each intermediate time point from a newly generated random distribution which depends on the end point of a

previous trajectory at that time. Furthermore, one now has to collect the generated data into a matrix of times t' and t'' so that finally the double time integration may be carried out using the trapezoid rule.

Although becoming complicated, the actual algorithm, up to order two is straightforward. The computation of the third-order term though is much more prohibitive, since now one would have two intermediate sets of phase space variables and would have to store a matrix for three times, so that the storage requirements may become critical. In principle this could be overcome by treating also the time integration using Monte Carlo methods, but to date we have not tested how well one could converge such a computation.

References

- (1) Miller, W. H. *J. Chem. Phys.* **1970**, *53*, 3578.
- (2) Heller, E. J. *J. Chem. Phys.* **1981**, *75*, 2923.
- (3) Herman, M. F.; Kluk, E. *Chem. Phys.* **1984**, *91*, 27.
- (4) Campolieti, G.; Brumer, P. *J. Chem. Phys.* **1992**, *96*, 5969.
- (5) Kay, K. G. *J. Chem. Phys.* **1994**, *100*, 4377.
- (6) Kay, K. G. *J. Chem. Phys.* **1994**, *100*, 4432.
- (7) Kay, K. G. *J. Chem. Phys.* **1994**, *101*, 2250.
- (8) Garaschuk, S.; Tannor, D. J. *Chem. Phys. Lett.* **1996**, *262*, 477.
- (9) Makri, N.; Thompson, K. *Chem. Phys. Lett.* **1998**, *291*, 101.
- (10) de Sand, G. v.; Rost, J. M. *Phys. Rev. A* **1999**, *59*, R1723.
- (11) Thompson, K.; Makri, N. J. *Chem. Phys.* **1999**, *110*, 1343.
- (12) Shao, J.; Makri, N. J. *Phys. Chem. A* **1999**, *103*, 7753.
- (13) Gelabert, R.; Giménez, X.; Thoss, M.; Wang, H.; Miller, W. H. *J. Chem. Phys.* **2001**, *114*, 2572.
- (14) Sun, X.; Miller, W. H. *J. Chem. Phys.* **1999**, *110*, 6635.
- (15) Tannor, D. J.; Garaschuk, S. *Annu. Rev. Phys. Chem.* **2000**, *51*, 553.
- (16) Thoss, M.; Wang, H.; Miller, W. H. *J. Chem. Phys.* **2001**, *114*, 9220.
- (17) Shalashilin, D. V.; Child, M. S. *J. Chem. Phys.* **2001**, *115*, 5367.
- (18) Wright, N. J.; Makri, N. J. *Phys. Chem. B* **2004**, *108*, 6816.
- (19) Grossmann, F. *Comments At. Mol. Phys.* **1999**, *34*, 141.
- (20) Baranger, M.; de Aguiar, M. A. M.; Keck, F.; Korsch, H. J.; Schellhaas, B. *J. Phys. A: Math. Gen.* **2001**, *34*, 7227.
- (21) Miller, W. H. *J. Phys. Chem. A* **2001**, *105*, 2942.
- (22) Elran, Y.; Brumer, P. *J. Chem. Phys.* **2004**, *121*, 6763.
- (23) Kunikeev, S. D.; Atilgan, E.; Taylor, H. S.; Kaledin, A. L.; Main, J. J. *J. Chem. Phys.* **2004**, *120*, 6478.
- (24) Shao, J.; Makri, N. J. *Phys. Chem. A* **1999**, *103*, 9479.
- (25) Maitra, N. T. *J. Chem. Phys.* **2000**, *112*, 531.
- (26) Gelabert, R.; Gimenez, X.; Thoss, M.; Wang, H.; Miller, W. H. *J. Phys. Chem. A* **2000**, *104*, 10321.
- (27) Harabati, C.; Rost, J. M.; Grossmann, F. *J. Chem. Phys.* **2004**, *120*, 26.
- (28) Guallar, V.; Batista, V. S.; Miller, W. H. *J. Chem. Phys.* **1999**, *110*, 9922.
- (29) Ankerhold, J.; Saltzer, M.; Pollak, E. *J. Chem. Phys.* **2002**, *116*, 5925.
- (30) Pollak, E.; Shao, J. J. *Phys. Chem. A* **2003**, *107*, 7112.
- (31) Zhang, S.; Pollak, E. *J. Chem. Phys.* **2003**, *119*, 11058.
- (32) Zhang, S.; Pollak, E. *Phys. Rev. Lett.* **2003**, *91*, 190201.
- (33) Zhang, S.; Pollak, E. *J. Chem. Phys.* **2004**, *121*, 3384.
- (34) Ovchinnikov, M.; Apkarian, V. A. *J. Chem. Phys.* **1996**, *105*, 10312.
- (35) Sun, X.; Miller, W. H. *J. Chem. Phys.* **1997**, *106*, 916.
- (36) Zhang, D.-H.; Pollak, E. *Phys. Rev. Lett.* **2004**, *93*, 140401.
- (37) Pollak, E.; Miret-Artés, S. *J. Phys. A* **2004**, *37*, 9669.
- (38) Zhang, D.-H.; Pollak, E. To be published.
- (39) Berne, B. J.; Thirumalai, D. *Annu. Rev. Phys. Chem.* **1986**, *7*, 401.
- (40) Ceperley, D. M. *Rev. Mod. Phys.* **1995**, *7*, 279.

CT0499074